

# Theoretical study of carbon double cones

Mirleide D. Lopes<sup>1</sup>, Sérgio Azevedo<sup>1,a</sup>, Fernando Moraes<sup>1</sup>, and Marcelo Machado<sup>2</sup>

<sup>1</sup> Departamento de Física, Universidade Federal da Paraíba, Caixa Postal 5008, João Pessoa, Pb, Brazil

<sup>2</sup> Departamento de Física, Universidade Federal de Pelotas, Caixa Postal 354, 96010-900 Pelotas, RS, Brazil

Received 11 September 2014 / Received in final form 12 November 2014

Published online 8 January 2015 – © EDP Sciences, Società Italiana di Fisica, Springer-Verlag 2015

**Abstract.** We have applied first-principles calculations, based on the density functional theory, to investigate the electronic structure of pure and nitrogen (N) and (B) doped carbon (C) cones and double cones in a hourglass shape. The relative number of  $sp^3$  bonds, together with apex rearrangement and growth environment, determine the energetic stability of these structures. The electronic structure calculations revealed that the  $sp^2/sp^3$  ratio defines the gap size for the non doped double cones. For the doped systems it was observed a gap reduction for one specific configuration and that this reduction is associated with the defects interaction. Densities of states (DOS) changes in response to the application of external electric fields were observed, with some double cones becoming metallic. Permanent electric dipole moments, equal to  $-1.2$  eÅ and  $-2.3$  eÅ, were calculated for the B and N doped double cones. The interaction of this electric dipole with the electric field application can be used to tune the electronic properties of these systems.

## 1 Introduction

Along the last decade, planar, curved and wrapped nanoscale structures, like graphene, fullerenes and nanotubes [1–3] have been subject of increasing scientific attention and strong technological interest due to their innovative structural, electronic and mechanical properties [4–9]. The incorporation of pentagonal atomic rings and other topological defects into the hexagonal network of carbon nanotubes increases the local curvature and can lead to the tubes closure. The cap structure depends on the species of the included defect, but generally it has the aspect of a conical surface, with electronic properties that are distinct from the bulk material [10]. Carbon nanocones were observed as nanotubes caps [11] and free-standing structures [12,13]. They are interesting materials for technological applications due to the presence of a particular structure with sharp tips, which provide specific electronic and mechanical properties.

In general, conical structures are classified according to their disclination angles, which can be positive or negative [14]. Theoretical calculations have been carried out to investigate the electronic structure and stability of carbon and boron-nitrogen compounds with positive disclination [15–18]. Usually, these materials present  $sp^2$  hybridization. However, it is possible to obtain conical structures (e.g. double cones) that display  $sp^3$  hybridization. Regarding the energetic stability, cones and double cones are competitive. With this point in mind, in the present contribution we apply first-principles calculations

to study the relative stability and electronic behavior of hypothetical carbon double cones. Also, the effect of substitutional boron or nitrogen impurities on the properties of such structures are investigated. Finally, we have analysed the behavior of these compounds in the presence of an external electric field ( $E_{field}$ ).

## 2 Methodology

Our calculations are based on the density functional theory [19] as implemented in the SIESTA code [20]. A recently introduced exchange correlation functional [21,22], based on the Román Pérez and Soler scheme [23], which allows a self consistent treatment of van der Waals interactions, is employed. We make use of normconserving pseudopotentials [24] in the Kleinman-Bylander factorized form [25,26] and a double basis set composed of finite range numerical atomic pseudofunctions enhanced with polarization orbitals. Spin polarization is included in all calculations. A real space grid is used with a mesh cut-off of 150 Ryd. All geometries were optimized so that the maximum force on any atom is less than 0.1 eV/Ång.

The structures investigated in this contribution are displayed in Figure 1: in Figure 1a it is shown a carbon cone with a single pentagon at its apex; in Figure 1b it is shown a double cone, denoted Model I (MI), formed by the connection of two cones as the ones showed in (a); in Figure 1c we have a double cone, Model II (MII), where the composing cones share a single pentagon; finally, in Figure 1d we have a Model II double cone, where substitutional B and N impurities occupy two different carbon

<sup>a</sup> e-mail: sazevedo@fisica.ufpb.br

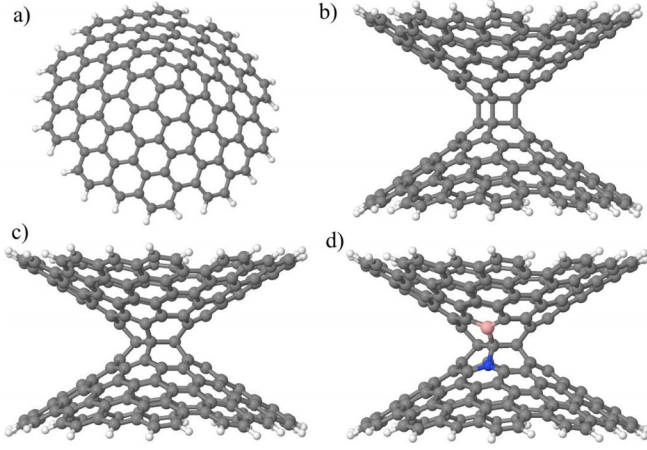


**Fig. 1.** Pictorial scheme of: (a) carbon nanocone, (b) carbon double cone Model I, (c) carbon double cone Model II, (d) carbon double cone doped with  $B_1N_2$  impurity. The carbon (C) atoms are represented by the gray spheres, while the boron (B) and nitrogen (N) atoms are stand for by pink and blue colors.

sites, one at each opposing cone. In all systems, the dangling bonds at the cones edges are saturated with hydrogen (H) atoms. The following nomenclature scheme was used in this work (see Tab. 1): (i) a B (N) indicates a substitutional boron (nitrogen) atom at a C site; (ii) the 1 (2) index indicates the substitution occurring at the upper (lower) cone or a C atom localized at the upper (lower) cone; (iii) rich-B (rich-N) indicates the growth chemical environment considered for the chemical potentials calculations.

### 3 Structural stability

The comparative analysis of the energetic stability of carbon nanocones saturated with hydrogen atoms are performed using a zero-temperature approach used on the prior determination of convenient chemical potentials, as described elsewhere [27–29]. In such approach, the formation energy,  $E_{form}$ , can be written as

$$E_{form} = E_{tot} - n_B\mu_B - n_C\mu_C - n_N\mu_N - n_{CH}\mu_{CH}, \quad (1)$$

where  $E_{tot}$  is the calculated total energy of the conical structures obtained from SIESTA,  $n_B$  and  $n_N$  are the number of boron and nitrogen atoms, respectively,  $n_C$  is the number of carbon atoms, and  $n_{HC}$  is the number of hydrogen-carbon pairs. Notice that in equation (1) we have used a finite carbon monolayer as reference, ascribing a null value to its formation energy.

Our first-principles results, for the formation energy of these structures, are shown in Table 1. It is possible to verify that the MI system is slightly more stable than MII (0.01 eV/atom). This behavior can be, partly explained if we compare the relative number of  $sp^3$  bonds at the apexes of the studied systems: Model II and I present, respectively, five and ten  $sp^3$  bonds. It is well known that  $sp^3$  bonds possess a stronger character, when compared to  $sp^2$

**Table 1.** Formation energy ( $E_{form}$ ) for the studied pristine and doped cones and double cones. At the third column we present the number of atoms of each system.

Structure	$E_{form}$ (eV/atom)	Atoms
Cone	0.342	140
double cone Model I	0.341	280
$B_1B_2$ (rich-B)	0.341	280
$B_1B_2$ (rich-N)	0.368	280
$B_1N_2$ (rich-B)	0.358	280
$B_1N_2$ (rich-N)	0.358	280
$N_1N_2$ (rich-B)	0.373	280
$N_1N_2$ (rich-N)	0.346	280
double cone Model II	0.351	275
$B_1B_2$ (rich-B)	0.352	275
$B_1B_2$ (rich-N)	0.379	275
$B_1N_2$ (rich-B)	0.365	275
$B_1N_2$ (rich-N)	0.365	275
$N_1N_2$ (rich-B)	0.376	275
$N_1N_2$ (rich-N)	0.350	275

ones. Another feature that should be taken into account, when thinking about the systems stability, is the geometric distortion at the cones apexes (due to the creation of a double cone). Comparing Models I and II we can see that, before geometric optimization, Model II maintains the original single cone disclination angle, atomic arrangement, and the C-C-C atomic angles (Fig. 1c), while Model I presents an unusual arrangement, with a cage-like configuration for the atoms at the apexes, presenting C-C-C angles equal to  $90^\circ$  (Fig. 1b). This should contribute to increase the double cone formation energy. However, it was observed a rearrangement of the atoms at the apex of system MI, after optimization. For example, the average value for the  $C_1C_2$  distance at the tip is  $1.62 \text{ \AA}$  (against  $\approx 1.44 \text{ \AA}$  for the C-C bond distance in the body of the cone). For this case we can say that we have two interacting cones instead of a double cone. This separation is even larger for  $B_1B_2$  MI, with the  $C_1C_2$  distance (close to the B atom) being around  $1.67 \text{ \AA}$  while the  $B_1B_2$  distance is equal to  $2.32 \text{ \AA}$ . Also, for the  $N_1N_2$  MI system we have  $1.70 \text{ \AA}$  for the  $C_1C_2$  distance (close to the N atom) and  $2.53 \text{ \AA}$  for the  $N_1N_2$  distance. This rearrangement (and cones separation) must be the responsible for the lowering in  $E_{form}$  for MI double cones, which should be higher for the non optimized structure seen in Figure 1b. For the MII double cones, we also see an atomic rearrangement at the apexes but no cones separation. The average C-C distance at the pentagonal ring at the apex is around  $1.61 \text{ \AA}$ , while is  $1.44 \text{ \AA}$  at the body of the cone (for the non doped system). For the  $B_1B_2$  MII double cone, at the apex, there is a little variation in the C-C bond distance being  $1.56 \text{ \AA}$  for the atoms close to the B atom and  $1.60 \text{ \AA}$  for the others. Finally, for the  $N_1N_2$  MII double cone, we see a more uniform distribution, with all C-C bond distances around  $1.61 \text{ \AA}$  at the pentagonal ring.

About the energies for the doped systems, it is well known that the inclusion of nitrogen or boron atoms in carbon conical structures might alter the energy cost for the formation of pentagonal rings [30,31]. In Table 1 we

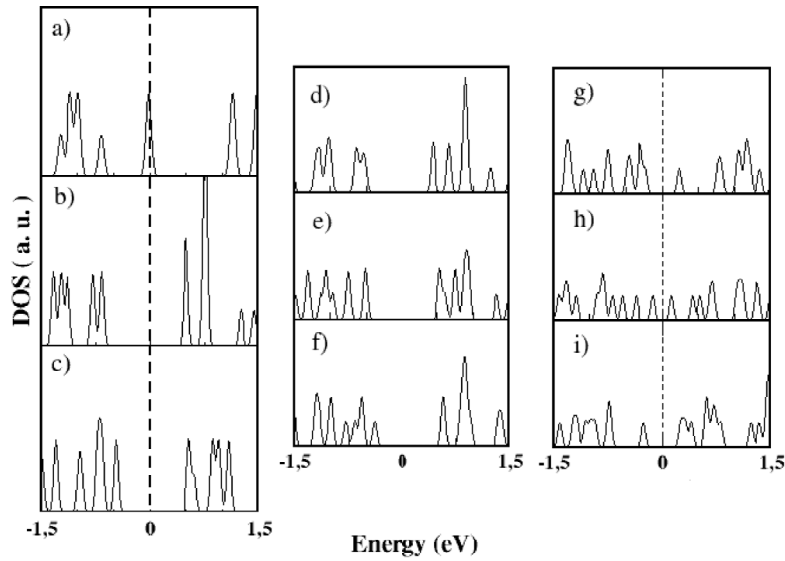


**Fig. 2.** Density of states for the studied structures. (a) Single C cone, (b) double cone MI, and (c) double cone MII. (d), (e), (f) The  $B_1B_2$ ,  $B_1N_2$ , and  $N_1N_2$  doped MI double cones, respectively. (g), (h), (i) The  $B_1B_2$ ,  $B_1N_2$ , and  $N_1N_2$  doped MII double cones, respectively. The Fermi level is represented by the dashed line.

present our results for the double cones formation energies with substitutional B and N atoms. Taking into account the results shown in Table 1 we can draw some general observations on the stability of boron and nitrogen doped carbon double cones. As expected, it is possible to verify that the most stable structure is  $B_1B_2$  (rich-B) Model I, followed closely by  $N_1N_2$  (rich-N) Model I. Also, the most unlikely structures to be growth in a synthesis process are the ones with substitutional B (N) atom in a N-rich (B-rich) environment. Finally, for the mixed cases ( $B_1N_2$  rich-B and rich-N) we have the same formation energy values. This indicates that one has the same difficulty to dope a B (N) atom in a rich-N (rich-B) environment. For Model II we observe the same pattern.

It is possible to calculate the energy barrier for the carbon double cones formation, using the following expression

$$E_{\text{barrier}} = E^{\text{double}} - E_1^{\text{isolated}} - E_2^{\text{isolated}}, \quad (2)$$

where  $E^{\text{double}}$  is the total energy of the double cone,  $E_1^{\text{isolated}}$  is the energy of one of the first isolated cone (which is half of the double one), and  $E_2^{\text{isolated}}$  is the total energy of the second isolated cone. From (2), we have obtained, for double cone Model I  $E_{\text{barrier}} = -2.04$  eV, while for double cone Model II we have  $E_{\text{barrier}} = 2.55$  eV. Therefore, considering that such double cones can be obtained from two isolated cones, it is possible to verify, from such results, that the double cone Model I is easier to be obtained than Model II. In addition, we can verify that these results are in accordance with those found for the formation energy, as can be seen in Table 1.

## 4 Electronic structure

The calculated densities of states (DOS) for the studied structures are illustrated in Figure 2. From Figure 2a, it

is possible to observe, in the case of a single carbon cone, the presence of a localized energy level in the Fermi energy ( $E_f$ ). Such state is associated to the odd number of bonds, due to the pentagonal ring at the cone apex. In a regular hexagonal network, each C atom is bonded to its neighbours by three sigma and one pi bond. With the inclusion of a pentagonal ring, in a perfect hexagonal lattice, we have one unpaired pi electron, which is associated with that localized energy level. This situation is automatically fixed for the double cones, with no unpaired electrons and hence no localized level near  $E_f$ .

In addition, we have observed alterations in the energy gap when going from the cone (1.81 eV) to the Model I (1.16 eV) and II (1.01 eV) double cones, as seen in Figures 2b and 2c. Namely, we have found that, despite the  $sp^3$  bonds inclusion and the absence of more delocalized  $p_z$  orbitals, the C double cones present a decrease at the gap energy when compared to single C cones. Also, when we compare double cones and single cones, there is an increase in the number of  $sp^3$  and  $sp^2$  bonds, however, the increase in the number of  $sp^2$  is much higher, which contributes to the decreasing of the gap. Besides, the  $sp^2/sp^3$  ratio is different in MI and MII, contributing to the gap differences between these systems. In addition, it was found that the single cone  $E_f$  localized state is shifted towards the valence band, inducing the gap reduction observed for the double cones. Still about these systems, spin polarized calculations revealed that they do not show unpaired electrons. For the double cones, for both systems, the inexistence of unpaired electrons is due to the tips interaction and the consequent introduction of  $sp^3$  bonds.

In Figures 2d to 2i it is shown the DOS for double cones MI and MII with substitutional B and N atoms. It is possible to verify that there is little alteration for MI system (Figs. 2d–2f). On the other hand,  $B_1B_2$ ,  $B_1N_2$ , and  $N_1N_2$  impurities induce significant modifications at the gap region for MII double cone (Figs. 2g–2i). In the

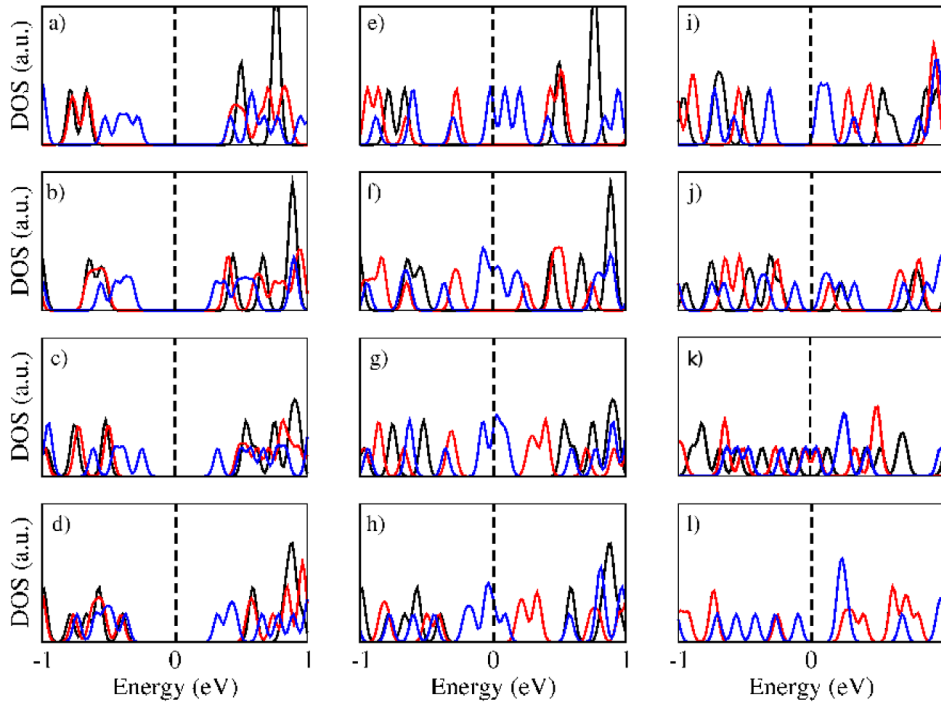


**Fig. 3.** Density of states of the studied double cones when subjected to external electric fields. (a) The non doped carbon double cone MI, (b) the  $B_1B_2$  MI, (c) the  $B_1N_2$  MI, (d)  $N_1N_2$  MI with the field applied perpendicularly to the double cones axis. (e)–(h) The same configurations and order but the field is applied parallelly to the double cones axis. (i) The non doped carbon double cone MII, (j) the  $B_1B_2$  MII, (k) the  $B_1N_2$  MII, and (l)  $N_1N_2$  MII with the field applied parallelly to the double cones axis. The solid black, red and blue lines are related to field magnitudes equal to 0, 0.1 V/Å, and 0.3 V/Å, respectively. The Fermi level is represented by the dashed line.

case of  $B_1B_2$  defects we have the introduction of two acceptor impurities at the system causing the shift of the valence band towards positive values and the inclusion of a localized level near  $E_f$  at the conduction band (Fig. 2g). On the other hand, when  $B_1N_2$  defects are introduced, we have the introduction of an acceptor (donor) state in the conduction (valence) band, with a consequent filling of the gap (Fig. 2h). In this case, we have a  $e-h$  pair, with a 0.1 eV binding energy, that is a important feature for optoelectronic devices. Finally, in the case of  $N_1N_2$  defects (donor impurities) we have the inclusion of a state in the valence band and a resulting shift of the conduction band towards negative values and a resulting gap closure. The differences in the electronic behavior, for the doped MI and MII double cones, can be associated to fact that in the MII, the distance between any defect is smaller than for any impurity in the MI.

We have also investigated the behavior of double cones when submitted to external electric fields, applied both perpendicularly and parallelly to the structures axis and with magnitudes equal to 0.1 and 0.3 V/Å. The densities of states for the studied systems are shown in Figure 3. Observing the left side of the Figures 3b–3d, we can notice that the behavior of MI systems is practically the same, when the field is applied in a direction that is perpendicular to the cones axis, with little variation for a field of 0.1 V/Å and a more pronounced filling of the gap when it is increased to 0.3 V/Å. For the non doped double

cone, we have measured an energy gap of  $\approx 0.55$  eV for a field equal to 0.3 V/Å, against  $\approx 0.98$  eV for a null  $E_{field}$ . For the  $B_1B_2$  MI double cone (Fig. 3b), as the result of a field application with magnitude equal to 0.3 V/Å, we have a gap reduction of about 0.33 eV, with a more pronounced filling of the valence band. With the substitution of one B for an N atom ( $B_1N_2$  MI, Fig. 3c), for the same field value we have a gap reduction of  $\approx 0.48$  eV, with a more balanced filling of both the valence and conduction bands. Finally, for the  $N_1N_2$  MI double cone (Fig. 3d), it was observed a gap reduction of 0.26 eV and a more pronounced filling of the conduction band for an external electric field equal to 0.3 V/Å. Now, for the same systems analysed above, but with the electric field applied in a direction parallel to the double cones axis (Figs. 3e–3h) we can see a more pronounced response to the application of a 0.1 V/Å field and also the filling of the gap for a field of 0.3 V/Å, with the structures becoming metallic. For the MII double cones we observed that, for the application of a perpendicular electric field, little alteration occurred at the DOS for all systems. However, when the field is applied parallelly to the double cones axis (Figs. 3i–3l) we can see some changes at the double cones DOS. In general, it is interesting to notice that, contrary to MI double cones, MII systems remain as semiconductors, for all the studied field magnitudes (exception being the  $B_1N_2$  system, as can be seen in Fig. 3k). Analysing the structures individually, for the non doped MII double cone it was

measured a considerable gap reduction of  $\approx 0.75$  eV when a field of  $0.3$  V/Å is applied, as shown in Fig. 3i). For this case, we have a final gap of  $\approx 0.13$  eV. Continuing, for the  $B_1B_2$  MII system, which already had a smaller energy gap (when compared to the non doped double cone), this reduction is smaller with the gap variation and the measured gap being, respectively,  $0.27$  and  $0.07$  eV (Fig. 3j). For the  $B_1N_2$  cone (Fig. 3k), we have a complete filling of the gap, for both external electric field magnitudes. This behavior can be associated with a combined shift of the valence (up) and conduction (down) bands for this double cone. Finally, for the  $N_1N_2$  MII double cone, we have observed no variation at the DOS for a field value of  $0.1$  V/Å (red line covering the black one), with the measured energy gap equal to  $0.40$  eV, while, with a field magnitude of  $0.3$  V/Å, the measured gap was  $0.19$  eV as can be seen in Figure 3l.

As the last analysis, we have calculated the permanent electric dipole moment for the B and N doped double cones. It was observed, for  $B_1N_2$  doped systems, the presence of a permanent electric dipole in the  $z$  direction with magnitude equal to  $-1.2$  eÅ for the MI double cone and  $-2.3$  eÅ for the MII structure, even for the no field situation. As a consequence, there is a greater gap variation (reduction) for the  $B_1N_2$  double cones (if compared to the other doped systems), when subjected to  $z$ -direction applied external electric fields. Besides, it was verified that, for electric fields applied in the  $z$ -direction, there was an increase of the energy gap, with the calculated values being  $0.11$ ,  $0.37$ , and  $0.38$  eV, for a field magnitude equal to  $0$ ,  $0.1$ , and  $0.3$  V/Å, respectively. In this manner, the controlled doping of substitutional B and N impurities of C double cones allied with the control of the applied field direction can be explored to tune the electronic properties of these nanometric composites which can be used as active parts of electronic devices.

We have also performed calculations for spin polarization of all structures here investigated. We have obtained that, in all cases, it does not exist any unpaired electron, therefore the net spin is null. Such behavior is due to the fact that the substitution of carbon atoms in the double cone is always in pairs, introducing a pair of extra electrons, a pair of extra holes or one electron-hole pair.

## 5 Conclusions

In summary, using first-principles calculations, we have found that, amongst the studied structures, the most stable ones were the pristine MI and the doped  $B_1B_2$  (rich-B) MI double cones, both presenting a formation energy equal to  $0.341$  eV/atom. It was seen that the energetic stability is related to the relative number of  $sp^2/sp^3$  bonds allied with geometric rearrangement of the structures apexes. Densities of states analysis have shown alterations at the MII double cones electronic structures due to the B and N doping, with a visible gap reduction for the  $B_1B_2$ ,  $B_1N_2$ , and  $N_1N_2$  systems. On the other hand, for the doped MI double cones little alteration is observed. This behavior is associated with a weak dopant interaction due to the

larger distance between the cones (if compared to the MI system). The alterations at the electronic structure of the double cones due to the application of external electric fields were investigated and it was seen that when the  $E_{field}$  is applied perpendicularly to the systems axis, there is a reduction of the energy gap for these double cones, which remain as semiconductors. On the other hand, with  $E_{field}$  applied parallelly to the double cones axis there is a complete filling of the band gap for the MI systems, while for the MII a remaining energy gap is observed, even for  $E_{field} = 0.3$  V/Å. The exception is the  $B_1N_2$  MII structure, which becomes metallic as the  $E_{field}$  is applied. This behavior is associated with the interaction of  $E_{field}$  with a permanent electric dipole moment ( $-2.3$  eÅ) calculated for this system, which is due to the presence of a B atom at one side of the double cone and a N atom at the other. In this sense, we conclude that boron and nitrogen doped carbon double cones subjected to external electric could be used as functional parts of electronic devices.

A recent work [32] called attention upon the behavior of a free quantum particle constrained to move in the surface of a double cone. Since the two cones are joined by a single point, the tip of both cones, the wavefunction of the particle is limited to either cone. The common tip acts as a filter, letting pass only particles with zero angular momentum. It will be very interesting then to study scattering in the discrete double cones presented in this contribution to see if sort of filter acts on the transmittance across the junction of the cones. This will appear in a forthcoming publication.

The authors would like to acknowledge the financial support from the Brazilian agencies CNPq, Capes/nanobiotec and INCT - Nanomateriais de Carbono.

## References

1. S. Ijima, Nature **354**, 56 (1991)
2. N. Hamada, S.I. Sawada, A. Oshiyama, Phys. Rev. Lett. **68**, 1579 (1992)
3. A. Rubio, J. Corkill, M.L. Cohen, Phys. Rev. B **49**, 5081 (1994)
4. F. Banhart, J. Kotakoski, A.V. Krasheninnikov, ACS Nano **5**, 26 (2011)
5. C.N.R. Rao, B.C. Satishkumar, A. Govindaraj, M. Nath. ChemPhysChem **2**, 78 (2001)
6. V.N. Popov, Mat. Sci. Eng. Rep. **43**, 61 (2004)
7. K. Balasubramanian, M. Burghard, Small **1**, 180 (2005)
8. H.W. Kroto, Nature **329**, 529 (1997)
9. A.K. Geim, K.S. Novoselov, Nat. Mater. **6**, 183 (2007)
10. S. Azevedo, M.S.C. Mazzoni, H. Chacham, R.W. Nunes, Appl. Phys. Lett. **82**, 2323 (2003)
11. S. Ijima, T. Ichibashi, Y. Ando, Nature **356**, 776 (1992)
12. M. Ge, K. Sattler, Appl. Phys. Lett. **64**, 710 (1994)
13. M. Ge, K. Sattler, Chem. Phys. Lett. **220**, 192 (1994)
14. S. Azevedo, Phys. Lett. A **337**, 431 (2005)
15. A. Cortijo, M.A.Z. Vozmediano, Nucl. Phys. B **763**, 293 (2007)

16. C. Furtado, F. Moraes, A.M. de M. Carvalho, Phys. Lett. A **372**, 5368 (2008)
17. S.P. Jordan, V.H. Crespi, Phys. Rev. Lett. **93**, 255504 (2004)
18. D. Pedreira, S. Azevedo, M. Machado, Phys. Rev. B **78**, 085427 (2008)
19. W. Kohn, L.J. Sham, Phys. Rev. **140**, A1133 (1965)
20. D. Sanchez-Portal, P. Ordejon, E. Artacho, J.M. Soler, Int. J. Quantum Chem. **65**, 453 (1997)
21. M. Dion, H. Rydberg, E. Schröder, D.C. Langreth, I.B. Lundqvist, Phys. Rev. Lett. **92**, 246401 (2004)
22. T. Thonhauser, V.R. Cooper, S. Li, A. Puzder, P. Hyldgaard, D.C. Langreth, Phys. Rev. B **76**, 125112 (2007)
23. G. Román Pérez, J.M. Soler, Phys. Rev. Lett. **103**, 096102 (2009)
24. N. Troullier, J.L. Martins, Phys. Rev. B **43**, 1993 (1991)
25. L. Kleinman, D.M. Bylander, Phys. Rev. Lett. **48**, 1425 (1982)
26. J.P. Perdew, K. Burke, M. Ernzerhof, Phys. Rev. Lett. **77**, 3865 (1996)
27. S. Azevedo, M.S.C. Mazzoni, R.W. Nunes, H. Chacham, Phys. Rev. B **70**, 205412 (2004)
28. S. Azevedo, J.R. Kaschny, Eur. Phys. J. B **86**, 395 (2013)
29. J.P. Guedes, S. Azevedo, M. Machado, Eur. Phys. J. B **80**, 135 (2011)
30. S. Azevedo, Phys. Lett. A **325**, 283 (2004)
31. G. Zhang, W. Dan, B. Gu, Appl. Phys. Lett. **80**, 2589 (2002)
32. K. Kowalski, J. Rembielinski, Ann. Phys. **329**, 146 (2012)